Article

Genetic Correlation, Pleiotropy, and Molar Morphology in a Longitudinal Sample of Australian Twins and Families

Kathleen S. Paul [1],*, Christopher M. Stojanowski [2], Toby Hughes [3], Alan H. Brook [3,4] and Grant C. Townsend [3],†

[1]   Department of Anthropology, University of Arkansas, Fayetteville, AR 72701, USA
[2]   Center for Bioarchaeological Research, School of Human Evolution and Social Change,
     Arizona State University, Tempe, AZ 85287, USA; christopher.stojanowski@asu.edu
[3]   Adelaide Dental School, The University of Adelaide, Adelaide, SA 5005, Australia;
     toby.hughes@adelaide.edu.au (T.H.); alan.brook@adelaide.edu.au (A.H.B.)
[4]   Barts and the London Dental Institute, Queen Mary University of London, London EC1M 6AX, UK
*   Correspondence: kspaul@uark.edu; Tel.: +1-479-718-1352
†   Posthumous contribution.

Abstract: This study aims to expand our understanding of the genetic architecture of crown morphology in the human diphyodont dentition. Here, we present bivariate genetic correlation estimates for deciduous and permanent molar traits and evaluate the patterns of pleiotropy within (e.g., m1–m2) and between (e.g., m2–M1) dentitions. Morphology was observed and scored from dental models representing participants of an Australian twin and family study (deciduous *n* = 290, permanent *n* = 339). Data collection followed Arizona State University Dental Anthropology System standards. Genetic correlation estimates were generated using maximum likelihood variance components analysis in SOLAR v.8.1.1. Approximately 23% of deciduous variance components models and 30% of permanent variance components models yielded significant genetic correlation estimates. By comparison, over half (56%) of deciduous–permanent homologues (e.g., m^2 hypocone–M^1 hypocone) were significantly genetically correlated. It is generally assumed that the deciduous and permanent molars represent members of a meristic molar field emerging from the primary dental lamina. However, stronger genetic integration among m2–M1/M2 homologues than among paired deciduous traits suggests the m2 represents the anterior-most member of a "true" molar field. The results indicate genetic factors act at distinct points throughout development to generate homologous molar form, starting with the m2, which is later replaced by a permanent premolariform crown.

Keywords: quantitative genetics; molar morphology; pleiotropy; dental development

1. Introduction

When it comes to dental diversity, mammals are unrivaled. Two conditions contribute to this diversity within individuals [1,2]. Most mammals are *heterodonts*, meaning their tooth rows include multiple tooth classes, each with distinct crown form: incisors, canines, premolars, and molars [3,4]. For many mammals, dental variation is also observed across an individual's lifespan; permanent teeth replace an initial set of deciduous teeth in a condition called *diphyodonty* [5–7]. The origins and underpinnings of these conditions have been considered using several lines of evidence, including embryology, experimental genetics, mathematical modeling, paleontology, and phylogenetics [6–13].

The field of quantitative genetics has also provided insight into these conditions, outlining the relative contribution of genes to tooth form and the coordination of genetic effects in determining dental phenotypes. In these efforts, pedigreed samples and relatedness coefficients approximate underlying additive genetic variation, which may (high *heritability* traits) or may not (low *heritability* traits) explain the structure of a corresponding dental data set—e.g., [14–21]. Quantitative genetic efforts also examine the potential for certain genetic effects to influence multiple dental characters (*pleiotropy*). With regard to understanding

the structure of mammalian dentitions, this work has provided crucial insight into the role of genes in partitioning the tooth row into distinct modules. While many studies have focused on tooth size in human and non-human primates [22–26], some efforts have centered around non-metric crown variants, shape variables, and cusp configuration [17,27–32].

Metric patterns have suggested genetic partitioning of distinct incisor and postcanine modules that may be highly conserved across mammals [23,25,27]. Submodularity (premolar/molar) in the postcanine dentition is also consistent with predictions outlined by Butler's morphogenetic field model [33–35]. However, a higher degree of genetic integration across fields has been reported for some primate populations [22,26]. The genetic architecture of human crown variation, in many cases, supports morphogenetic field effects, with the anterior-most member of each field characterized by higher heritability estimates [26] and traits expressed on neighboring teeth characterized by high genetic correlation estimates [31]. While patterns are not entirely consistent across mammalian taxa, quantitative genetic work has been essential to probing the foundations of heterodonty by examining the role of genes in structuring tooth form across the arcade.

Recent work has also focused on within-individual variation throughout ontogeny by considering the diphyodont (deciduous and permanent) dental complex as a cohesive entity. Heritability estimates for crown morphology suggest, on average, a moderately strong and stable contribution of genes to morphological variation across arcades (maxillary–mandibular) and across dentitions (deciduous–permanent), which may explain the high correspondence in crown form between primary and replacement teeth [19]. Recent findings also suggest this continuity is due, in part, to the reuse of genes throughout development to replicate crown form.

Recently, the authors reported genetic correlations for anterior crown morphology in a longitudinal dental sample of Australian twins and families [36]. Pleiotropy was indicated for few (<10%) deciduous incisor and canine character pairs and nearly one third of permanent incisor and canine pairs. In contrast, significant genetic correlations were reported for the majority (~70%) of deciduous–permanent homologues. These results implicate genetic factors in the conservation of incisor and, especially, canine crown form across an individual's span of dental development and the transition from deciduous to permanent teeth [36]. The findings provide important insight into the maintenance of distinct morphogenetic fields throughout crown development and tooth replacement in humans.

Yet to be explored is the genetic architecture of morphology of the diphyodont *postcanine* tooth row. Although heritability estimates have been reported for crown characters of the deciduous and permanent molars [19], genetic correlations have yet to be established. This represents a considerable gap in our understanding of dental variation, which the present study aims to address (see Research Aims and Hypotheses below).

The postcanine tooth row is a unique region of the human diphyodont dental complex. In the anterior dentition, primary incisors and canines are shed and replaced by larger permanent elements that are nearly identical in overall shape and morphology. In contrast, the postcanine dentition consists of deciduous molars, which are shed and replaced by permanent premolars [37–39]. The first deciduous molars could be considered premolariform, sharing select morphological similarities with their permanent successors; the second deciduous molars, however, look like smaller versions of the first permanent molars [40–42]. Another important distinction between the anterior and postcanine dentitions involves their dental laminae precursors. All deciduous teeth originate from the primary dental lamina, while their permanent successors originate from the secondary dental lamina [43]. The permanent molars, however, are unique in that: (a) they are the only teeth to develop from the primary dental lamina that are not exfoliated and later replaced, and (b) they are the only permanent teeth that do not have deciduous precursors [40,44–46]. Therefore, it may be more appropriate to consider the deciduous and permanent molars to be part of a cohesive primary postcanine field.

Research Aims and Hypotheses

The aim of this study is to examine the structure of additive genetic contributions to postcanine crown variation in the diphyodont dentition, with a focus on crown morphology. Here, our interest is in quantifying the degree to which the same genetic effects contribute to variation in distinct morphological characters within a sample of known relatives. To achieve this goal, we generated a series of quantitative genetic models to estimate bivariate genetic correlations (ρ_G) for deciduous and permanent molar morphology. The analyses test the following null hypotheses:

1. Paired deciduous traits are genetically independent of one another: dtrait1–dtrait2 $\rho_G = 0$; dtrait1–dtrait2 $\rho_G \neq 1$ (no pleiotropy).
2. Paired permanent traits are genetically independent of one another: PTrait1–PTrait2 $\rho_G = 0$; PTrait1–PTrait2 $\rho_G \neq 1$ (no pleiotropy).
3. Paired deciduous/permanent traits are genetically independent of one another: dtrait1–PTrait1 $\rho_G = 0$; dtrait1–PTrait1 $\rho_G \neq 1$ (no pleiotropy).

2. Materials and Methods

Materials and methods follow those outlined in Paul et al. (2021). Molar morphology data were collected for 25 deciduous crown traits and 38 permanent crown traits referencing the University of Adelaide Twin Study (UAT) dental cast collection (n = 290 subadults; n = 339 adults). The UAT represents nearly forty years of data collection with over 1200 twins and 2000 relatives (as of 2014) enrolled as participants from the regions surrounding Adelaide, South Australia and Melbourne, Victoria [47].

Sampling for the current study targeted individuals included in UAT Cohort 2, [47–49], a longitudinal subset of the broader study. Cohort 2 members were recruited through the Australia National Health and Medical Research Council's registry of monozygotic (MZ) and dizygotic (DZ) twins; members of the twins' immediate families were also invited to participate [47–49]. Dental casts for Cohort 2 represent three key phases of participants' dental development: (1) deciduous dentition, (2) mixed dentition (i.e., a combination of deciduous and permanent teeth present in the oral cavity), and (3) permanent dentition. If the teeth of twins' parent(s) or an older sibling were molded and casted, typically only phase 3 would be represented for those individuals.

The present study sample includes individuals spanning over 100 nuclear families, the majority of which would be characterized as European–Australian with respect to ancestry or bioregional affiliation—see [19,36,47]. Genealogy information indicates that extended relationships (beyond nuclear family) are limited if not absent from the study. As such, kinship pairs are characterized as MZ twin, DZ twin, full-sibling, half-sibling, or parent-offspring. Individuals belonging to different families were assumed to be non-relatives, approximating randomly sampled members of a broad population—following [19,36,47].

Although UAT dental casts were assigned unique identifiers, during data collection individuals and families were recoded using a study-specific numbering system. This further preserved subject anonymity—see [19,36]. Research design and protocols were reviewed by Arizona State University's Institutional Review Board, the University of Adelaide School of Dentistry, and the Craniofacial Biology and Dental Education Research Group (see IRB Statement).

2.1. Data Collection Methods

Morphological data collection followed standards outlined by the Arizona State University Dental Anthropology System (ASUDAS) [50,51]. The traits included in this study and their respective abbreviations are shown in Table 1. Per this system, each crown character's expression was quantified as an ordinal "grade" on both left and right sides of the dentition [51]. ASUDAS reference plaques were used during data collection, and expression was scored from stone casts with the aid of supplemental lighting. While the ASUDAS was formulated for permanent morphology, these standards have been successfully employed in previous investigations of deciduous crown variation with moderately low intraobserver

error rates—see Results and [19,36]. Ultimately, all M3 traits were eliminated from the study due to restricted representation of M3s in the cast sample.

Table 1. Morphological crown traits for UAT data collection.

Morphological Trait [1]	Abbreviation	Dental Elements Scored
Metacone	META	m^1, m^2, M^1, M^2, M^3
Hypocone	HYPO	m^1, m^2, M^1, M^2, M^3
Cusp 5 (*Metaconule*) [2]	C5	m^1, m^2, M^1, M^2, M^3
Carabelli's Trait [2]	CTRAIT	m^1, m^2, M^1, M^2, M^3
Parastyle [2]	PARA	m^1, m^2, M^1, M^2, M^3
Anterior Fovea [2]	AFOV	m_1, m_2, M_1
Deflecting Wrinkle	DWRINK	m_2, M_1
Cusp 5 (*Hypoconulid*)	C5	m_1, m_2, M_1, M_2, M_3
Cusp 6	C6	m_1, m_2, M_1, M_2, M_3
Cusp 7 [2]	C7	m_1, m_2, M_1, M_2, M_3
Cusp Number	CNO	m_1, m_2, M_1, M_2, M_3
Groove Pattern	GROOVE	m_2, M_1, M_2, M_3
Protostylid [2]	PSTYLID	m_1, m_2, M_1, M_2, M_3
Distal Trigonid Crest	DTCREST	m_2, M_1, M_2, M_3

[1] Maxillary and mandibular arcades are indicated by superscripts and subscripts, respectively. [2] Scoring standards were augmented for observation on the first deciduous molar, but data were ultimately removed due to lack of precision in data recording. These m1 traits are not necessarily homologous to the permanent characters upon which the scoring standards are based.

2.2. Analytical Methods

2.2.1. Observer Error

To test for intraobserver error, a subset (~20%) of the original sample was rescored eight or more weeks after initial data collection—see [19]. Raw grade differences between data recording sessions were referenced to ensure that any existing error was not systematic. Absolute grade differences were calculated [52] to examine the full magnitude of between-session error. Quantitative genetic analyses were performed on all morphological variables for which average intraobserver error fell below 0.30 grades. Results for models involving traits characterized by an error range greater than 1 grade were conservatively flagged and interpreted with caution—following [36].

Morphological variants were separated into three distinct variables prior to analysis: (1) left side expression, (2) right side expression, and (3) maximum expression [19,36]. For the maximum expression variable, each individual was represented by either left or right antimere data for each trait based on differential observability (whichever side is present and observable) or expression (whichever side is associated with the highest degree of trait expression).

2.2.2. Quantitative Genetic Modeling

Maximum likelihood variance components analysis was used to generate a suite of parameter values, including narrow-sense heritability and bivariate genetic, environmental, and (derived) phenotypic correlations. These methods have been outlined in previous publications [18,26,31,32], with narrow-sense heritability and genetic correlations for the anterior dentition recently reported for this sample [19,36]. Variance components analysis utilizes documented genealogical and demographic data (age, sex, household) to isolate fixed and random effects while modeling the variance/covariance structure of a phenotypic data set—in this case, molar crown morphology [53,54]. For the analyses, pedigree and demographic data were obtained from UAT records. Twin pairs were assigned unique numbers with zygosity listed based on UAT documentation [47].

Bivariate genetic correlation models were generated using SOLAR v.8.1.1 [55,56], a software that models phenotypic covariance as:

$$\Omega = G \, Y \, 2\Phi + E \, Y \, I$$

where Ω: trait (co)variance matrix; G: genetic (co)variance matrix; Y: Kronecker product operator; Φ: kinship matrix; E: environmental (co)variance matrix; and I: identity matrix. Parameter estimates generated for each model include genetic correlation (ρ_G), environmental correlation (ρ_E), and derived phenotypic correlation (ρ_P)—see [36] for ρ_P equation.

For each bivariate trait pair, separate models were generated for likelihood comparison: (1) all parameter values freely estimated, and (2) parameter of interest held constant (model 2a: $\rho_G = 0$; model 2b: $|\rho_G| = 1$). For the genetic correlation parameter, significant difference ($\alpha = 0.05$) in likelihood between model 1 and model 2a is interpreted as complete pleiotropy. Significant difference in likelihood between model 1 and both model 2a and 2b is interpreted as incomplete pleiotropy—following [26,28,29,31].

For analytical purposes, ordinal variables were treated as continuous, with *inorm* data transformation applied to limit violation of distributional assumptions where appropriate—see [19,36]. This approach is justified by current understandings of ASUDAS trait expression (i.e., Liability or Threshold Models), in which morphological characters are quasi-continuous with latent genetic potential following a normal distribution and observed phenotypic variation binned into discrete categories as dictated by population-level genetic "thresholds" for expression [57–64]. Further support for this approach comes from findings that variation in tooth number and size also conforms to a quasi-continuous statistical model with thresholds. From these results a unifying model has been constructed and further developed to include tooth shape [65,66]. Several demographic covariates were considered (sex, age, and sex*age interaction) and fixed when their mean effects were deemed significant (conservatively, $p \leq 0.10$) in initial variance components models of univariate heritability—see Tables S1 and S2 [19,36].

3. Results

3.1. Observer Error Results

Certain deciduous traits were removed from the study because they were monomorphic (m[1] cusp 5) for this sample or because the traits are likely non-homologous with the permanent molar characters upon which scoring standards are based (m[1] Carabelli's trait, m[1] parastyle, m[1] anterior fovea, m[1] protostylid, and m[1] cusp 7) (Table 1). This is due to m1's premolariform crown and not the specific scoring system employed. Deciduous and permanent groove pattern were also eliminated because the data structure for these traits is categorical as opposed to ordinal (Y pattern, X pattern, + pattern).

Maximum intraobserver error ranged from 0–1 grade for the majority of traits scored. Those characterized by error outside of this range include: m^1/M^1 metacone, m^1/M^1 parastyle, M_1 anterior fovea, m_1/M_2 cusp 7 (for all, maximum error = 2 grades), and m_2/M_2 protostylid (maximum error = 3 grades). Of these traits, only m_2/M_2 protostylid were omitted from the genetic correlation analysis based on error results, as all other listed traits are associated with mean error values less than 0.30. Additionally, as reported in Paul et al. (2020), error data for m^1 metacone (binomial probability = 0.03), M_1 anterior fovea (binomial probability = 0.02), and M^1 parastyle (binomial probability = 0.01) showed observation session biases—either all error session scores were lower or higher than the original scores. Results are presented for associated models but flagged for interpretive purposes (Tables S1 and S2).

3.2. Genetic Correlation Results

Genetic correlation results for paired antimeres are presented in Table 2. Correlation estimates are high for all traits, with many approaching or equaling 1.0. Complete pleiotropy is indicated for all left/right paired deciduous traits. Antimeric trait pairs in the permanent dentition show strong integration with few exceptions. No pleiotropy is indicated for M^2 paracone, M_2 cusp 6, or M_2 distal trigonid crest. Note that models for these traits are flagged for interpretive purposes, because the standard deviation ranges for certain parameters were incalculable or problematic. As more M1s than M2s were available for data collection, these models were also characterized by relatively small sample sizes.

Table 2. Antimeric variance component correlations.

Trait [1]	N/Cov [2]	Genetic ρ_G [3]	$P(\rho_G = 0)$ [4]	$P(\lvert\rho_G\rvert = 1)$ [4]	Environmental ρ_E [5]	$P(\rho_E = 0)$ [4]	Phenotypic ρ_P [6]
DECIDUOUS (l−r)							
m^1 meta [e]	249	0.978 ± 0.077 **	**<0.001**	0.387	−0.144 ± 0.131	0.283	0.597
m^2 meta	278/a	0.852 ± 0.094 **	**<0.001**	0.057	−0.144 ± 0.111	0.208	0.434
m^1 hypo [w]	251	1.000 ± − **	**<0.001**	−	0.114 ± 0.106	0.282	0.642
m^2 hypo	279	0.992 ± 0.056 **	**<0.001**	0.445	0.005 ± 0.112	0.967	0.648
m^2 c5	272/s	0.868 ± 0.087 **	**<0.001**	0.070	0.132 ± 0.140	0.345	0.625
m^2 ctrait [w]	276	1.000 ± − **	**<0.001**	−	0.227 ± 0.112	**0.046**	0.758
m^2 para	278	1.000 ± − **	**<0.001**	−	0.263 ± 0.117	**0.021**	0.638
m_2 afov	268	0.753 ± 0.139 **	**<0.001**	0.053	0.182 ± 0.120	0.134	0.446
m_2 dwrink	261	1.000 ± − **	**<0.001**	−	−0.152 ± 0.118	0.228	0.607
m_1 c5	239/s	1.000 ± − **	**<0.001**	−	−0.085 ± 0.125	0.501	0.578
m_2 c5	281/a, a*s	0.875 ± 0.176 **	**0.001**	0.249	0.173 ± 0.120	0.161	0.412
m_1 c6 [w]	−	−	**—**	−	−	−	−
m_2 c6 [cf]	−	−	**—**	−	−	−	−
m_2 c7	283	0.938 ± 0.054 **	**<0.001**	0.120	0.107 ± 0.121	0.374	0.687
m_1 cno [w]	239/s	1.000 ± − **	**<0.001**	−	0.020 ± 0.126	0.871	0.591
m_2 cno [cf]	−	−	−	−	−	−	−
m_2 dtcrest [w]	253/a	1.000 ± − **	**<0.001**	−	0.269 ± 0.185	0.179	0.492
PERMANENT (L−R)							
M^1 META [E]	327	1.000 ± − **	**<0.001**	−	0.221 ± 0.095	**0.028**	0.555
M^2 META	151/S, A*S	0.990 ± 0.232 **	**0.002**	0.483	0.544 ± 0.127	**<0.001**	0.668
M^1 HYPO	319/S	1.000 ± − **	**<0.001**	−	−0.206 ± 0.108	0.073	0.620
M^2 HYPO	112	1.000 ± − **	**<0.001**	−	−0.523 ± 0.312	0.276	0.878
M^1 C5	292/A, A*S	0.968 ± 0.051 **	**<0.001**	0.263	−0.085 ± 0.143	0.558	0.675
M^2 C5 [W]	117	1.000 ± − **	**<0.001**	−	−0.498 ± 0.220	0.095	0.596
M^1 CTRAIT	302/A, A*S	0.965 ± 0.032 **	**<0.001**	0.119	0.438 ± 0.100	**<0.001**	0.801
M^2 CTRAIT	135/A, A*S	0.792 ± 0.100 *	**<0.001**	**0.023**	0.056 ± 0.257	0.828	0.641
M^1 PARA [E]	314	0.886 ± 0.110 **	**<0.001**	0.148	−0.429 ± 0.118	**0.001**	0.306
M^2 PARA [W]	154	0.093 ± −	1.000	0.500	0.440 ± −	**<0.001**	0.439
M_1 AFOV [E]	294/A, A*S	1.000 ± − **	**<0.001**	−	−0.098 ± 0.155	0.528	0.655
M_1 DWRINK	301	0.973 ± 0.059 **	**<0.001**	0.324	−0.278 ± 0.112	**0.023**	0.580
M_1 PSTYLID	293/S	0.916 ± 0.100 **	**<0.001**	0.207	0.282 ± 0.158	0.103	0.605
M_1 C5	280/ALL	0.935 ± 0.046 *	**<0.001**	0.062	−0.149 ± 0.131	0.275	0.696
M_2 C5 [W]	145/S	1.000 ± − **	**<0.001**	−	0.290 ± 0.249	0.283	0.784
M_1 C6	281/A*S	1.000 ± − **	**<0.001**	−	0.152 ± 0.114	0.183	0.512
M_2 C6 [W]	144	−0.075 ± −	1.000	0.500	−0.018 ± −	0.878	−0.018

Table 2. *Cont.*

		Genetic			Environmental		Phenotypic
Trait [1]	N/Cov [2]	ρ_G [3]	$P(\rho_G = 0)$ [4]	$P(\|\rho_G\| = 1)$ [4]	ρ_E [5]	$P(\rho_E = 0)$ [4]	ρ_P [6]
PERMANENT (L−R)							
M_1 C7	330/S	1.000 ± − **	**<0.001**	−	0.144 ± 0.134	0.263	0.694
M_2 C7 [E]	187	1.000 ± − **	**0.047**	−	0.182 ± 0.152	0.269	0.368
M_1 CNO	293	1.000 ± − **	**<0.001**	−	0.233 ± 0.111	**0.039**	0.588
M_2 CNO	140	0.991 ± 0.092 **	**<0.001**	0.462	−0.144 ± 0.308	0.653	0.695
M_1 DTCREST [W]	300/S	0.327 ± − *	**<0.001**	**<0.001**	1.000 ± −	**<0.001**	0.338
M_2 DTCREST [W]	182	0.900 ± −	1.000	1.000	0.920 ± −	1.000	0.920

[1] l/L = left; r/R = right; m/M = molar. Maxillary and mandibular traits indicated by superscript and subscript, respectively. Deciduous and permanent indicated by lowercase and uppercase script, respectively. For a list of morphological trait abbreviations, see Table 1. "e/E" superscript indicates a trait that was originally flagged for intra-observer error because the error range exceeded a single grade but whose mean error does not exceed 0.300. Traits with mean error exceeding 0.300 were omitted from the correlation analyses. All third molar traits were omitted from the correlation analyses due to sample size limitations. "w/W" superscript indicates models that are suspect due to standard deviation ranges for certain estimates. "cf/CF" superscript indicates model convergence failure. [2] Covariates fixed in the genetic correlation models based on univariate model results (see Paul et al., 2020). "a/A" = age; "s/S" = sex; "a*s/A*S" = age/sex interaction; all/ALL = all covariates. [3] Maximum-likelihood estimate of genetic correlation. Cases of incomplete pleiotropy indicated by a single asterisk. Cases of complete pleiotropy indicated by two asterisks. Dashes are associated with incalculable parameter estimates. [4] Probability of hypothesis (as indicated in parentheses) given pedigree structure with values $p < 0.050$ bolded. Dashes are associated with incalculable parameter estimates. [5] Maximum-likelihood estimate of environmental correlation. Dashes are associated with incalculable parameter estimates. [6] Maximum-likelihood estimate of derived phenotypic correlation. Dashes are associated with incalculable parameter estimates.

For all other permanent left/right trait pairs, some degree of pleiotropy is indicated—incomplete for M^2 Carabelli's trait and M_1 distal trigonid crest and complete for all other characters. These results suggest significant genetic redundancy driving bilateral symmetry in postcanine crown morphology and justify the practice of collapsing left/right paired data sets. For the subsequent intertrait genetic correlation analyses, maximum expression data were analyzed, which served to increase sample size for each model.

Postcanine genetic correlations were calculated within dentitions (Tables S1–S2). Deciduous results are shown in Table S1 and indicate limited genetic integration for morphology of the deciduous molars. Approximately 23% of the quantitative genetic model results are significant, which is beyond the expectations of family-wise error at $\alpha = 0.10$. Most of these models show incomplete pleiotropic relationships between paired traits, with the exception of m_1 cusp number–m_1 cusp 5; significance testing for this model yielded values consistent with complete pleiotropy (Figure 1).

Of the trait pairs characterized by incomplete pleiotropy, nearly half are expressed on the same tooth crown: m^1 metacone–m^1 hypocone, m^2 metacone–m^2 cusp 5, m^2 hypocone–m^2 cusp 5, m^2 hypocone–m^2 Carabelli's trait, m^2 hypocone–m^2 paracone, m^2 cusp 5–m^2 Carabelli's trait, m^2 Carabelli's trait–m^2 paracone, m_2 anterior fovea–m_2 distal trigonid crest, m_2 deflecting wrinkle–m_2 cusp 7, and m_2 cusp 7–m_2 distal trigonid crest. Of note, pleiotropy is indicated for one metameric pair: m^1 hypocone–m^2 hypocone (Figure 1).

Genetic correlations for deciduous molars are both positive and negative in value (mean $\rho_G = 0.11$; absolute mean $\rho_G = 0.16$) (see Table S1). While within-arcade correlation values are stable across the dentition (maxillary mean $\rho_G = 0.14$; maxillary absolute mean $\rho_G = 0.19$; mandibular mean $\rho_G = 0.12$; mandibular absolute mean $\rho_G = 0.19$), genetic correlations for morphological isomeres are weaker (maxillary/mandibular mean $\rho_G = 0.09$; maxillary/mandibular absolute mean $\rho_G = 0.14$). Of the significant models, genetic correlations were positive for all but three: m^2 metacone–m^2 cusp 5, m^2 hypocone–m_2 anterior fovea, and m_2 cusp5–m_2 distal trigonid crest (Figure 1).

	m¹ meta	m² meta	m¹ hypo	m² hypo	m² c5	m² Ctrait	m² para	m₂ afov	m₁ cno	m₂ dwrink	m₁ c5	m₂ c5	m₂ c7	m₂ dtcrest
m¹ meta		0.08	0.38	0.04	−0.03	0.06	−0.04	0.32	0.03	0.00	0.12	−0.05	−0.11	0.22
m² meta	n		0.14	0.13	−0.29	0.06	−0.05	0.19	0.06	−0.04	0.11	0.36	−0.12	0.01
m¹ hypo	i	n		0.49	0.02	0.35	−0.06	0.01	0.32	0.32	0.46	−0.11	0.15	0.31
m² hypo	n	n	i		0.38	0.31	0.28	−0.32	0.26	0.16	0.29	0.34	0.16	−0.02
m² c5	n	i	n	i		0.25	0.12	0.33	−0.03	0.13	−0.02	0.06	0.05	0.16
m² Ctrait	n	n	i	i	i		0.38	−0.06	−0.06	−0.02	0.07	−0.10	0.08	−0.02
m² para	n	n	n	i	n	i		0.01	−0.11	0.35	−0.03	−0.01	0.18	0.03
m₂ afov	n	n	n	i	n	n	n		0.10	0.08	0.13	0.11	0.03	0.37
m₁ cno	n	n	i	n	n	n	n	n		0.24	0.94	−0.17	0.06	0.16
m₂ dwrink	n	n	i	n	n	n	i	n	n		0.12	0.00	0.32	0.08
m₁ c5	n	n	i	i	n	n	n	n	c	n		0.09	0.09	−0.04
m₂ c5	n	n	i	i	n	n	n	n	n	n	n		0.25	−0.45
m₂ c7	n	n	n	n	n	n	n	n	n	i	n	n		0.12
m₂ dtcrest	n	n	i	n	n	n	n	i	n	n	i	n	n	

Figure 1. Genetic correlation matrix for deciduous molar morphology. Correlation estimates are shown above the diagonal with positive values nonitalicized and negative values italicized. Cells are shaded based on absolute estimate values (<0.3 = light green; 0.3–0.6 = green; >0.6 = dark green). Pleiotropy-based model likelihood results are shown below the diagonal (n = no pleiotropy; i = incomplete pleiotropy; c = complete pleiotropy). Cells are shaded based on degree of pleiotropy (n = light yellow; i = yellow; c = dark yellow). Model results for within-arcade trait pairs are enclosed in boxes. Maxillary trait pairs are outlined with a solid line and mandibular trait pairs are outlined with a dotted line. For trait names and abbreviations, see Table 1.

Genetic correlation results for the permanent dentition are presented in Table S2. For permanent molar morphology, 30% of models yielded significant results, which is beyond the expectations of family-wise error at $\alpha = 0.10$. Three trait pairs are completely pleiotropic, and all involve cusp 7: M^1 paracone–M_2 cusp 7, M_1 protostylid–M_2 cusp 7, and M_1 cusp 7–M_2 cusp 7 (Figure 2). The remaining 47 significant models indicate incomplete pleiotropic relationships, many of which (19%) involve traits expressed on the same tooth crown (M^1: metacone–hypocone, hypocone–cusp 5, hypocone–Carabelli's trait, cusp 5–Carabelli's trait; M^2: hypocone–Carabelli's trait; M_1: cusp number–cusp 6, anterior fovea-deflecting wrinkle, cusp 5–cusp 6; M_2: cusp number–cusp 5).

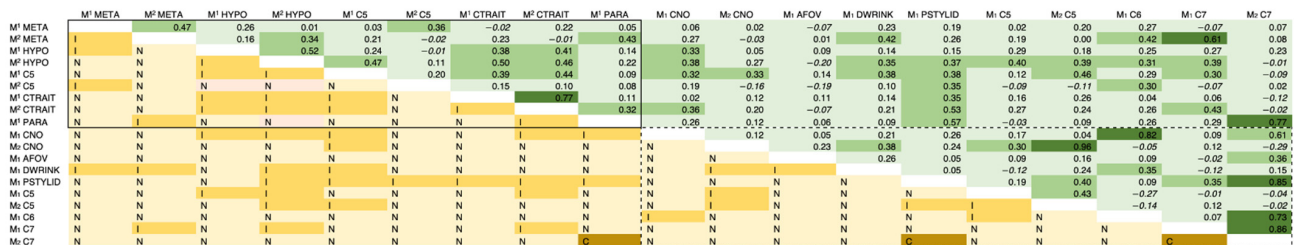|	M¹ META	M² META	M¹ HYPO	M² HYPO	M¹ C5	M² C5	M¹ CTRAIT	M² CTRAIT	M¹ PARA	M₁ CNO	M₂ CNO	M₁ AFOV	M₁ DWRINK	M₁ PSTYLID	M₁ C5	M₂ C5	M₁ C6	M₁ C7	M₂ C7
M¹ META		0.47	0.26	0.01	0.03	0.36	−0.02	0.22	0.05	0.06	0.02	−0.07	0.23	0.19	0.20	0.20	0.27	−0.07	0.07
M² META	I		0.16	0.34	0.21	−0.02	0.23	−0.01	0.43	0.27	−0.03	0.01	0.42	0.26	0.19	0.00	0.42	0.61	0.08
M¹ HYPO	I	N		0.52	0.24	−0.01	0.38	0.41	0.14	0.33	0.05	0.09	0.14	0.15	0.29	0.18	0.25	0.27	0.23
M² HYPO	N	N	I		0.47	0.11	0.50	0.46	0.22	0.38	0.27	−0.20	0.35	0.37	0.40	0.39	0.31	0.39	−0.01
M¹ C5	N	N	N	N		0.20	0.39	0.44	0.09	0.32	0.33	0.14	0.38	0.12	0.46	0.29	0.30	0.30	−0.09
M² C5	N	I	N	N	N		0.15	0.10	0.08	0.19	−0.16	−0.19	0.10	0.35	−0.09	−0.11	0.30	−0.07	0.02
M¹ CTRAIT	N	N	I	I	I	N		0.77	0.11	0.02	0.12	0.11	0.14	0.35	0.16	0.26	0.04	0.06	−0.12
M² CTRAIT	N	N	I	I	I	N	N		0.32	0.36	0.20	−0.07	0.21	0.53	0.27	0.24	0.26	0.43	−0.02
M¹ PARA	N	I	N	N	N	N	N	I		0.26	0.12	0.06	0.09	−0.57	−0.03	0.09	0.26	0.29	−0.77
M₁ CNO	N	N	N	N	I	N	N	N	I		0.12	0.05	0.21	0.26	0.17	0.04	0.82	0.09	0.61
M₂ CNO	N	N	N	N	N	N	N	N	N	N		0.23	0.38	0.24	0.30	0.98	−0.05	0.12	−0.29
M₁ AFOV	N	N	N	N	N	N	N	N	N	N	N		0.26	0.05	0.09	0.16	0.09	−0.02	0.36
M₁ DWRINK	N	I	N	N	I	N	N	N	I	N	N	N		0.05	−0.12	0.24	0.35	−0.12	0.15
M₁ PSTYLID	N	N	I	N	I	N	I	I	I	N	N	N	I		0.19	0.40	0.09	0.35	0.86
M₁ C5	N	N	N	I	N	N	I	I	N	I	N	N	N	N		0.19	0.40	0.09	−0.04
M₂ C5	N	N	N	I	N	N	N	N	N	N	N	N	N	N	I		0.43	−0.27	−0.01
M₁ C6	N	N	N	N	N	N	N	N	N	I	N	N	N	N	N	N		0.07	0.73
M₁ C7	N	I	N	I	N	N	N	I	N	N	N	N	N	N	I	N	N		0.86
M₂ C7	N	N	N	N	N	N	N	C	N	N	N	N	N	C	N	N	N	C	

Figure 2. Genetic correlation matrix for permanent molar morphology. Correlation estimates are shown above the diagonal with positive values nonitalicized and negative values italicized. Cells are shaded based on absolute estimate values (<0.3 = light green; 0.3–0.6 = green; >0.6 = dark green). Pleiotropy-based model likelihood results are shown below the diagonal (N = no pleiotropy; I = incomplete pleiotropy; C = complete pleiotropy). Cells are shaded based on degree of pleiotropy (N = light yellow; I = yellow; C = dark yellow). Model results for within-arcade trait pairs are enclosed in boxes. Maxillary trait pairs are outlined with a solid line, and mandibular trait pairs are outlined with a dotted line. For trait names and abbreviations, see Table 1.

Genetic redundancy is also indicated for the vast majority of metameric trait pairs, including: metacone, hypocone, Carabelli's trait, cusp 5 (mandibular), and cusp 7. This is a consistent pattern, considering that genetic correlations were not estimated between neighboring teeth for paracone, cusp 6, protostylid, or distal trigonid crest, while deflecting wrinkle and anterior fovea are only scored on a single tooth. For all other significant models, the patterns appear idiosyncratic, although M^1/M^2 hypocone and M_1 protostylid account for over 40% of the pleiotropic relationships (Figure 2).

Permanent molar models, like their primary counterparts, yielded both positive and negative genetic correlations (mean $\rho_G = 0.20$; absolute mean $\rho_G = 0.23$) (Table S2). Again,

within-arcade bivariate correlation is fairly stable across the maxillary (mean ρ_G = 0.22; absolute mean ρ_G = 0.25) and mandibular (mean ρ_G = 0.21; absolute mean ρ_G = 0.26) dentitions, while these values are slightly lower for isomerically paired characters (mean ρ_G = 0.19; absolute mean ρ_G = 0.21). Significant models yielded positive estimates with one exception: M_1 cusp 5–M_1 cusp 6 (Figure 2).

The results of the deciduous–permanent genetic correlation analyses are presented in Table 3. These include only metameric m2, M1, and M2 traits, as m1 morphology more closely resembles that of the replacement tooth (permanent P1) than other postcanine elements derived from the primary dental lamina. Deciduous–permanent homologues are moderately genetically integrated, with 56% of models yielding significant results, a markedly greater percentage than in the deciduous and permanent dentitions alone. For all significant models, incomplete pleiotropy is indicated; none of the deciduous–permanent trait pairs are characterized by complete genetic redundancy.

Table 3. Variance components correlations: paired deciduous and permanent morphology.

		Genetic			**Environmental**		**Phenotypic**
Trait [1]	**N/Cov** [2]	ρ_G [3]	$P\,(\rho_G = 0)$ [4]	$P\,(\lvert\rho_G\rvert = 1)$ [4]	ρ_E [5]	$P\,(\rho_E = 0)$ [4]	ρ_P [6]
Meta (m^2-M^1) [E]	355/Y	0.189 ± 0.158	0.230	**<0.001**	0.099 ± 0.148	0.502	0.147
Meta (m^2-M^2)	344/Y	0.183 ± 0.186	0.315	**<0.001**	−0.239 ± 0.155	0.142	0.003
Hypo (m^2-M^1)	352/N	0.597 ± 0.089 *	**<0.001**	**<0.001**	0.126 ± 0.140	0.370	0.460
Hypo (m^2-M^2)	332/N	0.445 ± 0.143 *	**0.006**	**<0.001**	−0.128 ± 0.441	0.776	0.346
C5 (m^2-M^1)	349/Y	0.547 ± 0.132 *	**<0.001**	**<0.001**	−0.323 ± 0.133	**0.032**	0.234
C5 (m^2-M^2)	326/Y	−0.157 ± 0.175	0.372	**<0.001**	0.483 ± 0.181	**0.034**	−0.062
CTrait (m^2-M^1)	354/Y	0.635 ± 0.075 *	**<0.001**	**<0.001**	0.040 ± 0.131	0.760	0.491
Ctrait (m^2-M^2)	337/N	0.368 ± 0.147 *	**0.019**	**<0.001**	−0.340 ± 0.186	0.099	0.253
Para (m^2-M^1) [E]	356/Y	0.239 ± 0.122	0.057	**<0.001**	0.265 ± 0.124	**0.043**	0.243
AFov (m_2-M_1) [E]	329/Y	0.691 ± 0.139 *	**<0.001**	**0.032**	−0.077 ± 0.138	0.583	0.353
DWrink (m_2-M_1)	332/N	0.520 ± 0.078 *	**<0.001**	**<0.001**	−0.016 ± 0.158	0.920	0.440
Pstylid (m_2-M_1) [E]	340/Y	0.659 ± 0.128 *	**<0.001**	**0.009**	−0.300 ± 0.132	**0.038**	0.300
C5 (m_2-M_1)	343/Y	0.168 ± 0.165	0.329	**0.008**	0.195 ± 0.138	0.170	0.146
C5 (m_2-M_2)	335/Y	−0.391 ± 0.240	0.109	**0.018**	0.502 ± 0.202	**0.050**	0.042

Table 3. *Cont.*

		Genetic			Environmental		Phenotypic
Trait [1]	**N/Cov** [2]	ρ_G [3]	$P\,(\rho_G = 0)$ [4]	$P\,(\lvert\rho_G\rvert = 1)$ [4]	ρ_E [5]	$P\,(\rho_E = 0)$ [4]	ρ_P [6]
C7 ($m_2 - M_1$)	352/Y	0.649 ± 0.154 *	**<0.001**	**0.027**	-0.234 ± 0.136	0.107	0.265
C7 ($m_2 - M_2$) [E]	345/Y	0.455 ± 0.240	0.056	0.071	-0.096 ± 0.214	0.657	0.180

[1] m/M = molar. Maxillary and mandibular traits indicated by superscript and subscript, respectively. Deciduous and permanent traits indicated by lowercase and uppercase script, respectively. All traits represented by their maximum antimeric expression score. For a list of morphological trait abbreviations, see Table 1. "E" superscript indicates a trait that was originally flagged for intra-observer error because the error range exceeded a single grade but whose mean error does not exceed 0.300. Traits with mean error exceeding 0.300 were omitted from the correlation analyses. All models involving m_2/M_2 cusp 6, m_2 cusp number, M^2 paracone, and M_1/M_2 distal trigonid crest either failed to converge or yielded suspect results due to standard deviation ranges for parameter estimates and are excluded from the table and all summary statistics. [2] Covariates fixed in the genetic correlation models based on univariate model results (see Paul et al., 2020). Only sex was fixed for deciduous–permanent homologue correlations due to the structure of the "age" data set. "N" = sex covariate not fixed; "Y" = sex covariate fixed. [3] Maximum-likelihood estimate of genetic correlation. Cases of incomplete pleiotropy indicated by a single asterisk. Dashes are associated with incalculable parameter estimates. [4] Probability of hypothesis (as indicated in parentheses) given pedigree structure with values $p < 0.050$ bolded. Dashes are associated with incalculable parameter estimates. [5] Maximum-likelihood estimate of environmental correlation. Dashes are associated with incalculable parameter estimates. [6] Maximum-likelihood estimate of derived phenotypic correlation. Dashes are associated with incalculable parameter estimates.

On average, deciduous–permanent metameres are more strongly correlated (mean $\rho_G = 0.36$; absolute mean $\rho_G = 0.43$). Interestingly, the results show weaker genetic correlation between maxillary deciduous–permanent homologues (mean $\rho_G = 0.36$; absolute mean $\rho_G = 0.36$) than between their mandibular counterparts (mean $\rho_G = 0.39$; absolute mean $\rho_G = 0.50$). All analyzed trait pairs are positively correlated with two exceptions: m^2–M^2 cusp 5 and m_2–M_2 cusp 5; pleiotropy is not indicated for these two models (Table 3).

4. Discussion

4.1. Morphology Versus Size

Considering both raw and absolute values, mean correlation for molar morphology (deciduous < 0.20 and permanent < 0.25) is similar to that reported for anterior dental morphology (deciduous < 0.21 and permanent < 0.23) in this sample. While this suggests stability in the degree of genetic redundancy occurring in distinct regions of the dentition, these values are markedly lower than reported averages for postcanine crown size in humans (maxillary = 0.73 and mandibular = 0.84) [26]. The same can be said for postcanine crown size correlations in callitrichid and cercopithecoid monkeys (tamarins: maxillary = 0.64 and mandibular = 0.73; macaques: maxillary = 0.50 and mandibular = 0.45; baboons: maxillary = 0.51 and mandibular = 0.46) [19,22,23,25], as well as mice (maxillary = 0.72 and mandibular = 0.72) [25]. This indicates that a greater degree of genetic redundancy underlies size data than morphology data collected from tooth crowns. This is not surprising, given the functional constraints on tooth size relating to occlusion, eruption, and the surrounding bony anatomy of the masticatory complex [67,68], although shape is not entirely exempt from these limitations [69]. It appears that genetic effects are efficiently deployed to meet these constraints—something that sets crown size apart from crown form.

Our results corroborate another reported difference between dental metric and morphological genetic architectures: genetic correlations are, with few exceptions [25], positive for metric traits but both positive and negative for morphological traits [19,22,23,26,31,32,36]. As reasoned in previous studies, this is likely due to the complex nature of crown morphology [31,32,36]. ASUDAS traits include variants that correspond with both negative and positive topographic features: cuspules, fissures, ridges, depressions, and crests, to name a few.

Moreover, these features occur on various surfaces of the tooth crown: lingual, buccal, occlusal, mesial, and distal [36]. It is not surprising that the same genes are implicated in multiple phenotypic outcomes, in some cases with corresponding effects (e.g., increase expression trait 1—increase expression trait 2) and, in other cases, with opposing effects (e.g., increase expression trait 1—decrease expression trait 2). We discuss negative correlations and potential interpretations in more detail below.

4.2. Antimeric Correlations and Bilateral Symmetry

Genetic correlation estimates for left–right paired traits suggest strong bilateral integration for molar morphology. Most values approach 1.0, with complete pleiotropy indicated for all deciduous and most permanent traits (Table 2). With the exception of M_2 cusp 6, all derived phenotypic correlations for left–right character pairs are positive and exceed 0.30. Together, these results affirm a tendency toward strong morphological symmetry in the molars, which—in nearly all cases—is driven by consistency in genetic effects. Similar results were obtained for anterior (incisor and canine) morphology in this sample [36] and for dental phenotypes observed in other human [26,31] and non-human primate samples [25]. These consistent findings across traits, populations and species empirically justify the standard anthropological practice of "collapsing" an individual's left and right side dental data to a single value per trait. In fact, to skip this step in a reconstruction of evolutionary relationships would almost certainly bias the analysis because it would lead to the inclusion of genetically redundant information.

However, we note that the only other quantitative genetic study of postcanine morphology reported limited symmetry in genetic effects, as interpreted from disparate left–right heritability estimates, limited genetic correlation, and moderate derived phenotypic correlation for paired characters [32]. This may reflect a sample-specific decoupling of genetic factors across antimeres, but it is also possible the patterns reported in Stojanowski et al. (2019) are the result of dichotomizing quasi-continuous trait variation to presence/absence (i.e., calculating genetic correlations between binary traits)—an approach that was not employed in the current study.

4.3. Within-Dentition Correlations (Deciduous–Deciduous and Permanent–Permanent)

Considering deciduous and permanent dentitions separately, molar morphology is minimally integrated. The deciduous molar analyses identified one completely pleiotropic trait pair: m_1 cusp number–m_1 cusp 5. This is not surprising, given that cusp 5 variation (namely, presence versus absence) directly influences variation in cusp number [50,51,70]. Therefore, this result reflects the mechanics of scoring these interdependent traits on a crown that typically possesses either four or five cusps [71,72].

In the permanent dentition, all cases of complete pleiotropy involve M_2 cusp 7. The genetic redundancy in M_1–M_2 cusp 7 is expected, given their metameric relationship, but the strong correlations between M_2 cusp 7–M^1 paracone and M_2 cusp 7–M_1 protostylid are difficult to interpret. These results may indicate that similar genes are involved in accessory cusp formation and crown elaboration along the buccolingual plane. Yet, if that is the case, it is unclear why similar results were not obtained for M_1 cusp 7.

Of the remaining traits that share some degree of genetic redundancy, many occur *on the same tooth*, which suggests a high degree of within-crown morphological integration. Although this pattern reflects a true biological phenomenon—overlapping genes implicated in manifold morphological outcomes—it also underscores the limitations of our methods for quantifying crown variation. By this, we mean that ultimate crown morphology is the result of developmental processes that are highly coordinated within a single tooth: oral epithelial–ectomesenchymal interactions, determination of placode location and size, enamel knot formation and placement, inner-enamel epithelial folding, and tissue (enamel) secretion—as reviewed in [73].

Experimental research has shown these processes are tightly controlled by (epi)genetic mechanisms that act on tooth crowns, and indeed the entire dentition, as cohesive enti-

ties [74–78]. Yet, current standards for quantifying morphological variation treat individual cusp size, crest presence, tubercle formation, and fissure patterning as isolated phenomena [50,51,79]. Researchers might adjust for this statistically by reducing multivariate morphological data sets to their "essential" components using PCA or PCoA. However, the ASUDAS bins variation into discrete "grades", for which imputation is generally not a valid approach when morphology is unobservable and data are missing [50,51]. In short, we are limited in our ability to probe the ways in which crown characters have correlated impacts on population variation because we lack methods for holistically measuring crown form. While computer automated approaches to dental phenomic profiling (e.g., geometric morphometrics, topography variables, complexity measures, sheering quotients, "fingerprinting") might yield alternatives to the ASUDAS, to date these methods have been restricted in their anthropological application, often to functional studies of diet or wear [80–88].

Another set of traits that accounts for a large portion of the significant model results includes *later-forming cusps of the upper molars*, especially hypocone, cusp 5, and Carabelli's trait. Of the deciduous traits that yielded valid model results, m^1 hypocone shares an incomplete pleiotropic relationship with ~54% percent of them. This result for m^2 hypocone is ~62% and ~32% for Carabelli's trait. M^1 hypocone shows significant genetic correlation with 39% of other permanent traits, while model results for M^2 hypocone (56%), M^1 cusp 5 (50%), and M^2 Carabelli's trait (50%) indicate incomplete pleiotropy for over half of the characters analyzed. This finding suggests that coordinated additive genetic effects play a major role in the developmental regulation of cusp size and presence in postcanine teeth.

The pattering cascade model provides a framework for interpreting these findings. It posits that cusp number and size (initially quantified as height but here quantified as area) are determined by: (a) overall size of the tooth germ, and (b) spatial patterning of enamel knots [89,90]. At the enamel–dentine junction, secondary enamel knots mark the site of future cusp tips and are surrounded by zones of inhibition, where signaling molecules regulate morphology by restricting formation of additional enamel knots [10,91–94]. In this way, homologous cusps and their positioning arise throughout crown formation via a dynamic reaction–diffusion process, where a shift in one secondary enamel knot might have a "cascade" effect altering overall tooth form [10,77,89,95]. In the maxillary molars, the cusps of the trigone (protocone, paracone, and metacone) are the earliest forming; the talon (hypocone) and accessory cusps (cusp 5, Carabelli's trait, and paracone) form latest or, in some cases, not at all [96–98]. Thus, the strong correlation between hypocone and other late-forming cusps may reflect coordinated gene regulation of cusp spacing dictated by earlier forming enamel knots. This interpretation is in line with those of previous applications of the patterning cascade model to human molar morphology [99,100].

This pattern is not as strong in the lower molars, however. Interestingly, in the permanent mandibular teeth, the later forming cusps (cusp 5 and cusp 6) are significantly correlated, but the correlation is *negative*. This suggests the same genes are implicated in lower cusp 5 and cusp 6 expression but their effects are opposing. A similar result was reported by Stojanowski and colleagues in their study of human molar morphology [32]. Their interpretation invoked previous research on life history traits that suggests negative genetic correlations reflect cases of within-organism resource competition across developmental processes [101–104].

Combining this insight with expectations outlined in the patterning cascade model, we might interpret the negative correlation between these neighboring cusps as competition for "cellular real estate" during morphogenesis and enamel secretion [13,32,89,105]. The key word is *neighboring*. The difference between cusp 5 and cusp 6 in the lower molars and most later-forming cusps of the upper molars is that cusps 5 and 6 are situated next to each other at the distal-most aspect of the crown. Thus, their sizes depend directly on relative enamel organ partitioning and the cellular territory allotted to their neighbor during crown formation [32]. The nature of this relationship is somewhat intuitive and reflected in data collection standards for cusp 6—this is one of the few traits for which

expression is based on size *relative* to another feature, in this case cusp 5 [50,51]. What these genetic correlation results provide, however, is greater insight into how development and (epi)genetic factors work in tandem to produce elaborate, multicuspid crown forms from fairly simple epithelial precursors.

4.4. Between-Dentition Correlations (Deciduous–Permanent)

As the UAT Cohort 2 sample is longitudinal with most individuals represented by deciduous and permanent dental casts, this study provides a unique opportunity to examine the morphological architecture of the diphyodont molar row. Because m1s are more similar in crown form to permanent premolars, we generated genetic correlations for homologous trait pairs of m2–M1 and m2–M2.

Raw and absolute genetic correlations are higher for paired deciduous–permanent molar traits (mean = 0.36 and absolute mean = 0.43) than for paired traits within dentitions (deciduous: mean = 0.11 and absolute mean = 0.16; permanent: mean = 0.20 and absolute mean = 0.23), with over half characterized by incomplete pleiotropy. This is a similar pattern to that observed in the anterior dentition for this sample, and it is tempting to draw a similar interpretation: that there is "a stronger genetic mechanism for morphological conservation across the diphyodont dentition than within individual tooth rows" [36]. However, we must consider the unique developmental trajectory shared by deciduous and permanent molars.

Unlike the incisors and canines, the permanent molar class is not succedaneous. That is to say, deciduous molars are replaced not by permanent molars but by permanent premolars. Permanent molars do not replace any primary elements and are the only permanent teeth to arise from the primary dental lamina—the same dental lamina from which all deciduous teeth originate [98]. Unlike incisors and canines, deciduous molars and their premolar successors have limited morphological variation in common, at least with respect to variants quantified using ASUDAS standards [50,51]. For this reason, it is more appropriate to treat deciduous and permanent molars as metameres: homologous structures of a single postcanine tooth row or molar field [106]—following [33,40,41,44,107].

That said, the stronger genetic correlation between m2 and the permanent molars corroborates previous research that suggests the m1 is, for lack of a better term, an oddity. The m1 is *somewhat* premolariform, but, compared to other elements, it does not strongly resemble any other tooth in the diphyodont dental complex. If considered part of a meristic molar field, this unique morphology is unexpected [40,44,96,108,109]. Further, despite its early crown completion, m1 is more variable in size and morphology than is m2 [110–112]. Previous researchers have suggested that m2 represents the "key tooth" of a cohesive molar field or, at a minimum, the deciduous postcanine field [40,111–113]. While these results do not provide direct support for this statement, the relatively weak genetic correlations between m1 and m2 traits indicate the molar field might contain only four "true" members: m2, M1, M2, and M3 [41,42,44]. However, we note that M3 data were ultimately omitted from the study due to sample size limitations.

4.5. Study Limitations

While we note several consistencies between these and previous quantitative genetic findings, sample composition and certain methodological choices may have impacted ultimate results. First, the reported genetic correlations represent a primarily European–Australian sample characterized by its own population-specific morphology profile. Previous research has shown morphological trends in both additive and non-additive genetic factors (for example, dominance for traits contributing to crown "complexity" and mass) that may result in disparate patterns for populations of distinct biogeographic origin [114].

Due to the UAT's recruitment strategy, this sample also includes a disproportionately large number of MZ twins, which sets it apart from broader pedigree/family study samples. Finally, as in our study of anterior morphology [36], morphological correlations were calculated from maximum expression (left or right) data for ordinal variables. It is possible

that genetic correlations calculated from dichotomized presence/absence data for the same characters might provide additional insight into the underlying genetic architecture of these quasi-continuous traits.

5. Conclusions

Within dentition (deciduous–deciduous and permanent–permanent) correlation values are, on average, lower than those estimated for homologous traits across dentitions (e.g., m^2 hypocone–M^1 hypocone). Further, a greater percentage of deciduous–permanent trait pairs exhibit some degree of redundancy in genetic effects (incomplete pleiotropy). As both the deciduous and permanent molars arise from the primary dental lamina, they likely represent elements of a meristic tooth district. Still, the relative degree of genetic integration noted for m2–M1–M2 morphology as compared to m1–m2 morphology aligns with previous suggestions that the m2 is the anterior-most member of a cohesive primary molar field. This is compatible with the overall distinctiveness of the m1 crown form.

Appendix A

Data were collected following ASUDAS standards (see Supplementary Materials Data .csv files) [51]. Scoring standards for certain traits include "half" grades (e.g., 3.5 for metacone and hypocone and 1A for cusp 7). These "half" grades were treated as full grades for the analysis. For example, metacone expression scores traditionally range from

0–5 [51]. In this data set, scores range from 0–6 because 3.5 is treated as a full grade. Data are presented for left (l/L) and right (r/R) sides and maximum antimeric expression (max/MAX). Maxillary traits are indicated with "x/X", and mandibular traits are indicated with "n/N".

References

1. Ungar, P.S. *Mammal Teeth: Origin, Evolution, and Diversity*; John Hopkins University Press: Baltimore, MD, USA, 2010. [CrossRef]
2. Ungar, P.S. Origins and functions of teeth: From "toothed" worms to mammals. In *A Companion to Dental Anthropology*; Irish, J.D., Scott, G.R., Eds.; John Wiley & Sons, Inc.: Chichester, UK, 2016; Chapter 3; pp. 21–36. [CrossRef]
3. Lumsden, A.G.S.; Osborn, J.W. The evolution of chewing: A dentist's view of palaeontology. *J. Dent.* **1977**, *5*, 269–287. [CrossRef]
4. Luo, Z.-X. Transformation and diversification in early mammal evolution. *Nature* **2007**, *450*, 1011–1019. [CrossRef]
5. Kielan-Jaworowska, Z.; Cifelli, R.L.; Luo, Z.-Z. *Mammals from the Age of Dinosaurs: Origins, Evolution, and Structure*; Columbia University Press: New York, NY, USA, 2004.
6. Luo, Z.-X.; Kielan-Jaworowska, Z.; Cifelli, R.L. Evolution of dental replacement in mammals. *Bull. Carnegie Mus. Nat. Hist.* **2004**, *36*, 159–175. [CrossRef]
7. Tucker, A.S.; Fraser, G.J. Evolution and developmental diversity of tooth regeneration. *Semin. Cell Dev. Biol.* **2014**, *25–26*, 71–80. [CrossRef]
8. Buchtová, M.; Stembírek, J.; Glocová, K.; Matalová, E.; Tucker, A.S. Early regression of the dental lamina underlies the development of diphyodont dentitions. *J. Dent. Res.* **2012**, *91*, 491–498. [CrossRef]
9. Cobourne, M.T.; Sharpe, P.T. Making up the numbers: The molecular control of mammalian dental formula. *Semin. Cell Dev. Biol.* **2010**, *21*, 314–324. [CrossRef]
10. Jernvall, J.; Thesleff, I. Tooth shape formation and tooth renewal: Evolving with the same signals. *Development* **2012**, *139*, 3487–3497. [CrossRef]
11. Townsend, G.; Harris, E.F.; Lesot, H.; Clauss, F.; Brook, A. Morphogenetic fields within the human dentition: A new, clinically relevant synthesis of an old concept. *Arch. Oral Biol.* **2009**, *54*, S43–S44. [CrossRef]
12. Tucker, A.S.; Matthews, K.; Sharpe, P.T. Transformation of tooth type by inhibition of BMP signalling. *Science* **1998**, *282*, 1136–1138. [CrossRef]
13. Weiss, K.M.; Stock, D.W.; Zhao, Z. Dynamic interactions and the evolutionary genetics of dental patterning. *Crit. Rev. Oral Biol. Med.* **1998**, *9*, 369–398. [CrossRef]
14. Biggerstaff, R.H. Heritability of the Carabelli's cusp in twins. *J. Dent. Res.* **1973**, *52*, 40–44. [CrossRef]
15. Dempsey, P.J.; Townsend, G.C. Genetic and environmental contributions to variation in human tooth size. *Heredity* **2001**, *86*, 685–693. [CrossRef]
16. Hardin, A.M. Genetic contributions to dental dimensions in brown-mantled tamarins (*Saguinus fuscicollis)* and rhesus macaques (*Macaca mulatta*). *Am. J. Phys. Anthropol.* **2019**, *168*, 292–302. [CrossRef]
17. Hlusko, L.J.; Mahaney, M.C. Genetic contributions to expression of the baboon cingular remnant. *Arch. Oral Biol.* **2003**, *48*, 663–672. [CrossRef]
18. Lawrence, J.; Stojanowski, C.M.; Paul, K.S.; Seidel, A.C.; Guatelli-Steinberg, D. Heterogeneous frailty and the expression of linear enamel hypoplasia in a genealogical population. *Am. J. Phys. Anthropol.* **2021**, *176*, 638–651. [CrossRef]
19. Paul, K.S.; Stojanowski, C.M.; Hughes, T.E.; Brook, A.H.; Townsend, G.C. Patterns of heritability across the human diphyodont dental complex: Crown morphology of Australian twins and families. *Am. J. Phys. Anthropol.* **2020**, *172*, 447–461. [CrossRef]
20. Townsend, G.C. Heritability of deciduous tooth size in Australian aboriginals. *Am. J. Phys. Anthropol.* **1980**, *53*, 297–300. [CrossRef]
21. Townsend, G.C.; Brown, T. Heritability of permanent tooth size. *Am. J. Phys. Anthropol.* **1978**, *49*, 497–504. [CrossRef]
22. Hardin, A.M. Genetic correlations in the dental dimensions of *Saguinus fuscicollis*. *Am. J. Phys. Anthropol.* **2019**, *169*, 557–566. [CrossRef]
23. Hardin, A.M. Genetic correlations in the rhesus macaque dentition. *J. Hum. Evol.* **2020**, *148*, 102873. [CrossRef]
24. Hlusko, L.J.; Mahaney, M.C. Quantitative genetics, pleiotropy, and morphological integration in the dentition of *Papio hamadryas*. *Evol. Biol.* **2009**, *36*, 5–18. [CrossRef]
25. Hlusko, L.J.; Sage, R.D.; Mahaney, M.C. Modularity in the mammalian dentition: Mice and monkeys share a common dental genetic architecture. *J. Exp. Zool. Part B Mol. Dev. Evol.* **2011**, *316*, 21–49. [CrossRef]
26. Stojanowski, C.M.; Paul, K.S.; Seidel, A.C.; Duncan, W.N.; Guatelli-Steinberg, D. Heritability and genetic integration of tooth size in the South Carolina Gullah. *Am. J. Phys. Anthropol.* **2017**, *164*, 505–521. [CrossRef]
27. Grieco, T.M.; Rizk, O.T.; Hlusko, L.J. A modular framework characterized micro- and macroevolution of Old World monkey dentitions. *Evolution* **2012**, *67*, 241–259. [CrossRef]
28. Hlusko, L.J.; Do, N.; Mahaney, M.C. Genetic correlations between mandibular molar cusp areas in baboons. *Am. J. Phys. Anthropol.* **2007**, *132*, 445–454. [CrossRef]
29. Hlusko, L.J.; Maas, M.-L.; Mahaney, M.C. Statistical genetics of molar cusp patterning in pedigreed baboons: Implications for primate dental development and evolution. *J. Exp. Zool. Part B Mol. Dev. Evol.* **2004**, *302*, 268–283. [CrossRef]

30. Koh, C.; Bates, E.; Broughton, E.; Do, N.T.; Fletcher, Z.; Mahaney, M.C.; Hlusko, L.J. Genetic integration of molar cusp size variation in baboons. *Am. J. Phys. Anthropol.* **2010**, *142*, 246–260. [CrossRef]

31. Stojanowski, C.M.; Paul, K.S.; Seidel, A.C.; Duncan, W.N.; Guatelli-Steinberg, D. Heritability and genetic integration of anterior tooth crown variants in the South Carolina Gullah. *Am. J. Phys. Anthropol.* **2018**, *167*, 124–143. [CrossRef]

32. Stojanowski, C.M.; Paul, K.S.; Seidel, A.C.; Duncan, W.N.; Guatelli-Steinberg, D. Quantitative genetic analyses of postcanine morphological crown variation. *Am. J. Phys. Anthropol.* **2019**, *168*, 606–631. [CrossRef]

33. Butler, P.M. Studies of the mammalian dentition, differentiation of the post-canine dentition. Differentiation of the post-canine dentition. *Proc. Zool. Soc. Lond.* **1939**, *B109*, 1–36. [CrossRef]

34. Dahlberg, A.A. The changing dentition of man. *J. Am. Dent. Assoc.* **1945**, *32*, 676–690. [CrossRef]

35. Dahlberg, A.A. The dentition of the American Indian. In *The Physical Anthropology of the American Indian*; Laughlin, W.S., Ed.; Viking Fund Inc.: New York, NY, USA, 1951; pp. 138–176.

36. Paul, K.S.; Stojanowski, C.M.; Hughes, T.E.; Brook, A.H.; Townsend, G.C. The genetic architecture of anterior tooth morphology in a longitudinal sample of Australian twins and families. *Arch. Oral Biol.* **2021**, *129*, 105168. [CrossRef]

37. AlQahtani, S.J.; Hector, M.P.; Liversidge, H.M. Brief communication: The London atlas of human tooth development and eruption. *Am. J. Phys. Anthropol.* **2010**, *142*, 481–490. [CrossRef]

38. Schour, I.; Massler, M. The development of the human dentition. *J. Am. Dent. Assoc.* **1941**, *28*, 1153–1160.

39. Smith, B.H. Standards of human tooth formation and dental age assessment. In *Advances in Dental Anthropology*; Kelley, M.A., Larsen, C.S., Eds.; Wiley-Liss: New York, NY, USA, 1991; pp. 143–168.

40. Bailey, S.E.; Benazzi, S.; Hublin, J.-J. Allometry, merism, and tooth shape of the upper deciduous and permanent M1. *Am. J. Phys. Anthropol.* **2014**, *154*, 104–114. [CrossRef]

41. Paul, K.S.; Astorino, C.M.; Bailey, S.E. The Patterning Cascade Model and Carabelli's trait expression in metameres of the mixed human dentition: Exploring a morphogenetic model. *Am. J. Phys. Anthropol.* **2017**, *162*, 3–18. [CrossRef]

42. Saunders, S.R.; Mayhall, J.T. Developmental patterns of human dental morphological traits. *Arch. Oral Biol.* **1982**, *27*, 45–49. [CrossRef]

43. Berkovitz, B.K.B.; Holland, G.R.; Moxham, B.J. *Oral Anatomy, Embryology, and Histology*, 4th ed.; Mosby International Ltd.: Edinburgh, UK, 2009.

44. Bailey, S.E.; Benazzi, S.; Buti, L.; Hublin, J.-J. Allometry, merism, and tooth shape of the lower second deciduous and first permanent molar. *Am. J. Phys. Anthropol.* **2016**, *159*, 93–105. [CrossRef]

45. Juuri, E.; Jussila, M.; Seidel, K.; Holmes, S.; Wu, P.; Richman, J.; Heikinheimo, K.; Chuong, C.-M.; Arnold, K.; Hochedlinger, K.; et al. Sox2 marks epithelial competence to generate teeth in mammals and reptiles. *Development* **2013**, *140*, 1424–1432. [CrossRef]

46. Olley, R.C.; Xavier, G.M.; Seppala, M.; Volponi, A.A.; Geoghegan, F.; Sharpe, P.T.; Cobourne, M.T. Expression analysis of candidate genes regulating successional tooth formation in the human embryo. *Front. Physiol.* **2014**, *5*, 445. [CrossRef]

47. Townsend, G.C.; Pinkerton, S.K.; Rogers, J.R.; Bockmann, M.R.; Hughes, T.E. *Twin Studies: Research in Genes, Teeth and Faces*; University of Adelaide Press: Adelaide, Australia, 2015. [CrossRef]

48. Hughes, T.; Bockmann, M.; Mihailidis, S.; Bennett, C.; Harris, A.; Seow, W.K.; Lekkas, D.; Ranjitkar, S.; Rupinskas, L.; LPinkerton, S.; et al. Genetic, epigenetic, and environmental influences on dentofacial structures and oral health: Ongoing studies of Australian twins and their families. *Twin Res. Hum. Genet.* **2013**, *16*, 43–51. [CrossRef]

49. Hughes, T.E.; Townsend, G.C.; Pinkerton, S.K.; Bockmann, M.R.; Seow, W.K.; Brook, A.H.; Richards, L.C.; Mihailidis, S.; Ranjitkar, S.; Lekkas, D. The teeth and faces of twins: Providing insights into dentofacial development and oral health for practising oral health professionals. *Aust. Dent. J.* **2014**, *59*, S101–S116. [CrossRef]

50. Scott, G.R.; Irish, J.D. *Human Tooth Crown and Root Morphology: The Arizona State Dental Anthropology System*; Cambridge University Press: Cambridge, UK, 2017. [CrossRef]

51. Turner, C.G., II; Nichol, C.R.; Scott, G.R. Scoring procedures for key morphological traits of the permanent dentition: The Arizona State University Dental Anthropology System. In *Advances in Dental Anthropology*; Kelly, M.A., Larsen, C.S., Eds.; Wiley-Liss: New York, NY, USA, 1991; pp. 13–31.

52. Nichol, C.R.; Turner, C.G. Intra- and interobserver concordance in classifying dental morphology. *Am. J. Phys. Anthropol.* **1986**, *69*, 229–315. [CrossRef]

53. Hopper, J.L.; Mathews, J.D. Extensions to multivariate normal models for pedigree analysis. *Ann. Hum. Genet.* **1982**, *46*, 373–383. [CrossRef]

54. Lange, K.; Boehnke, M.; Opitz, J.M. Extensions to pedigree analysis. IV. Covariance components models for multivariate traits. *Am. J. Med. Genet.* **1983**, *14*, 513–524. [CrossRef]

55. Almasy, L.; Blangero, J. Multipoint quantitative-trait linkage analysis in general pedigrees. *Am. J. Hum. Genet.* **1998**, *62*, 1198–1211. [CrossRef]

56. Blangero, J.; Lange, K.; Almasy, L.; Dyer, T.; Göring, H.; Williams, J.; Peterson, C. *SOLAR: Sequential Oligogenic Linkage Analysis Routine*; Version 8.1.1; Southwest Foundation for Biomedical Research: San Antonio, TX, USA, 1995–2016.

57. Harris, E.F. Anthropologic and Genetic Aspects of the Dental Morphology of Solomon Islanders, Melanesia. Ph.D. Thesis, Arizona State University, Tempe, AZ, USA, 1977.

58. Scott, G.R. Dental Morphology: A Genetic Study of American White Families and Variation in Living Southwest Indians. Ph.D. Thesis, Arizona State University, Tempe, AZ, USA, 1973.

59. Pilloud, M.A.; Edgar, H.J.H.; George, R.; Scott, G.R. Dental morphology in biodistance analysis. In *Biological Distance Analysis*; Pilloud, M.A., Hefner, J.T., Eds.; Academic Press: London, UK, 2016; pp. 109–133. [CrossRef]

60. Scott, G.R.; Pilloud, M.A. Dental morphology. In *Biological Anthropology of the Human Skeleton*, 3rd ed.; Katzenberg, A., Grauer, A.L., Eds.; Wiley-Liss: New York, NY, USA, 2018; pp. 257–292. [CrossRef]

61. Cheverud, J.M. Genetic and Environmental Morphological Variation among Social Groups of Rhesus Monkeys (*Macaca mulatta*) on Cayo Santiago. Ph.D. Thesis, University of Wisconsin, Madison, WI, USA, 1979.

62. Falconer, D.S. *Introduction to Quantitative Genetics*; Oliver & Boyd: Edinburgh, UK, 1960.

63. Falconer, D.S. The inheritance of liability to certain diseases from the incidence among relatives. *Ann. Hum. Genet.* **1965**, *29*, 51–76. [CrossRef]

64. Grüneberg, H. *The Pathology of Development*; Wiley: New York, NY, USA, 1963.

65. Brook, A.H. A unifying aetiological explanation for anomalies of tooth number and size in humans. *Arch. Oral Biol.* **1984**, *29*, 373–378. [CrossRef]

66. Brook, A.H.; O'Donnell, M.; Hone, A.; Hart, E.; Hughes, T.; Smith, R.N.; Townsend, G.C. General and craniofacial development are complex adaptive processes influenced by diversity. *Aust. Dent. J.* **2014**, *59*, 13–22. [CrossRef]

67. Gómez-Robles, A.; Polly, P.D. Hominin dentition: Evolutionary, developmental, and functional factors. *Evolution* **2012**, *66*, 1024–1043. [CrossRef]

68. Kieser, J.A.; Groeneveld, H.T. Tooth size and arcadal length correlated in man. *Int. J. Anthropol.* **1987**, *2*, 37–46. [CrossRef]

69. Evans, A.R.; Sanson, G.D. The tooth of perfection: Functional and spatial constraints on mammalian tooth shape. *Biol. J. Linn. Soc.* **2003**, *78*, 173–191. [CrossRef]

70. Scott, G.R.; Maier, C.; Heim, K. Identifying and recording key morphological (nonmetric) crown and root traits. In *A Companion to Dental Anthropology*; Irish, J.D., Scott, G.R., Eds.; John Wiley & Sons, Inc.: Hoboken, NJ, USA, 2015; pp. 245–264. [CrossRef]

71. Hanihara, K. Crown characters of the deciduous dentition of the Japanese-American hybrids. In *Dental Anthropology*; Brothwell, D.R., Ed.; Pergamon Press: London, UK, 1963; pp. 105–124. [CrossRef]

72. Sciulli, P.W. Evolution of the dentition in prehistoric Ohio Valley Native Americans II. Morphology of the deciduous dentition. *Am. J. Phys. Anthropol.* **1998**, *106*, 189–205. [CrossRef]

73. Lesot, H.; Brook, A.H. Epithelial histogenesis during tooth development. *Arch. Oral Biol.* **2009**, *54*, S25–S33. [CrossRef]

74. Balic, A.; Thesleff, I. Chapter Seven—Tissue interactions regulating tooth development and renewal. *Curr. Top. Dev. Biol.* **2015**, *115*, 157–186. [CrossRef]

75. Bei, M. Molecular genetics of tooth development. *Curr. Opin. Genet. Dev.* **2009**, *19*, 504–510. [CrossRef]

76. Brook, A.H. Multilevel complex interactions between genetic, epigenetic and environmental factors in the aetiology of anomalies of dental development. *Arch. Oral Biol.* **2009**, *54*, S3–S17. [CrossRef]

77. Jernvall, J.; Thesleff, I. Reiterative signaling and patterning during mammalian tooth morphogenesis. *Mech. Dev.* **2000**, *92*, 19–29. [CrossRef]

78. Sharpe, P.T. Neural crest and tooth morphogenesis. *Adv. Dent. Res.* **2001**, *15*, 4–7. [CrossRef]

79. Edgar, H.J.H.; Daly, E.S. *Dental Morphology for Anthropology: An Illustrated Manual*; Routledge: New York, NY, USA, 2017. [CrossRef]

80. Bunn, J.M.; Boyer, D.M.; Lipman, Y.; St. Clair, E.; Jernvall, J.; Daubechies, I. Comparing Dirichlet normal surface energy of tooth crowns, a new technique of molar shape quantification for dietary inference, with previous methods in isolation and combination. *Am. J. Phys. Anthropol.* **2011**, *145*, 247–261. [CrossRef]

81. Gaboutchian, A.V.; Knyaz, V.A.; Novikov, M.M.; Vasilyev, S.V.; Leybova, N.A.; Korost, D.V.; Cherebylo, S.A.; Kudaev, A.A. Automated digital odontometry: Measurement data analyses in cases of complicated dental morphology. *Int. Arch. Photogramm. Remote Sens. Spat. Inf. Sci.* **2020**, *XLIII*, B2. [CrossRef]

82. Kullmer, O.; Benazzi, S.; Fiorenza, L.; Schulz, D.; Bacso, S.; Winzen, O. Technical note: Occlusal fingerprint analysis: Quantification of tooth wear patterns. *Am. J. Phys. Anthropol.* **2009**, *139*, 600–605. [CrossRef] [PubMed]

83. Kullmer, O.; Benazzi, S.; Schulz, D.; Gunz, P.; Kordos, L.; Begun, D.R. Dental arch restoration using tooth macrowear patterns with application to *Rudapithecus hungaricus*, from the late Miocene of Rudabánya, Hungary. *J. Hum. Evol.* **2013**, *64*, 151–160. [CrossRef] [PubMed]

84. Pampush, J.D.; Winchester, J.M.; Morse, P.E.; Vining, A.Q.; Boyer, D.M.; Kay, R.F. Introducing molaR: A new R package for quantitative topographic analysis of teeth (and other topographic surfaces). *J. Mamm. Evol.* **2016**, *23*, 397–412. [CrossRef]

85. Silvester, C.M.; Hillson, S. A critical assessment of the potential for structure-from-motion photogrammetry to produce high fidelity 3D dental models. *Am. J. Phys. Anthropol.* **2020**, *173*, 381–392. [CrossRef]

86. Skinner, M.M.; Evans, A.; Smith, T.; Jernvall, J.; Tafforeau, P.; Kupczik, K.; Olejniczak, A.J.; Rosas, A.; Radovčić, J.; Thackery, J.F.; et al. Brief communication: Contributions of enamel-dentine junction shape and enamel deposition to primate molar crown complexity. *Am. J. Phys. Anthropol.* **2010**, *142*, 157–163. [CrossRef]

87. Winchester, J.M. MorphoTester: An open source application for morphological topographic analysis. *PLoS ONE* **2016**, *11*, e0147649. [CrossRef] [PubMed]

88. Yong, R.; Ranjitkar, S.; Townsend, G.C.; Smith, R.N.; Evans, A.R.; Hughes, T.E.; Lekkas, D.; Brook, A.H. Dental phenomics: Advancing genotype to phenotype correlations in craniofacial research. *Aust. Dent. J.* **2014**, *59*, 34–47. [CrossRef] [PubMed]

89. Jernvall, J. Linking development with generation of novelty in mammalian teeth. *Proc. Natl. Acad. Sci. USA* **2000**, *97*, 2641–2645. [CrossRef]

90. Jernvall, J.; Jung, H.-S. Genotype, phenotype, and developmental biology of molar tooth characters. *Yearb. Phys. Anthropol.* **2000**, *43*, 171–190. [CrossRef]

91. Jernvall, J.; Åberg, T.; Kettunen, P.; Keränan, S.; Thesleff, I. The life history of an embryonic signaling center: BMP-4 induces p21 and is associated with apoptosis in the mouth tooth enamel knot. *Development* **1998**, *125*, 161–169. [CrossRef]

92. Jernvall, J.; Kettunen, P.; Karavanova, I.; Martin, L.B.; Thesleff, I. Evidence for the role of the enamel knot as a control center in mammalian tooth cusp formation: Non-dividing cells express growth stimulating Fgf-4 gene. *Int. J. Dev. Biol.* **1994**, *38*, 463–469. [CrossRef]

93. Keränen, S.; Åberg, T.; Kettunen, P.; Thesleff, I.; Jernvall, J. Association of developmental regulatory genes with the development of different molar tooth shapes in two species of rodents. *Dev. Genes Evol.* **1998**, *208*, 477–486. [CrossRef]

94. Thesleff, I.; Sharpe, P. Signalling networks regulating dental development. *Mech. Dev.* **1997**, *67*, 111–123. [CrossRef]

95. Zhao, Z.; Weiss, K.M.; Stock, D.W. Development and evolution of dentition patterns and their genetic basis. In *Development, Function, and Evolution of Teeth*; Teaford, M., Smith, M.M., Ferguson, M., Eds.; Cambridge University Press: Cambridge, UK, 2000; pp. 152–172. [CrossRef]

96. Butler, P.M. The ontogeny of molar pattern. *Biol. Rev.* **1956**, *31*, 30–69. [CrossRef]

97. Christensen, G.J.; Kraus, B.S. Initial calcification of the human permanent first molar. *J. Dent. Res.* **1965**, *44*, 1338–1342. [CrossRef]

98. Kraus, B.S.; Jordan, R.E. *The Human Dentition Before Birth*; Lea Febiger: Philadelphia, PA, USA, 1965.

99. Hunter, J.P.; Guatelli-Steinberg, D.; Weston, T.C.; Durner, R.; Betsinger, T.K. Model of tooth morphogenesis predicts Carabelli cusp expression, size, and symmetry in humans. *PLoS ONE* **2010**, *5*, e11844. [CrossRef]

100. Moormann, S.; Guatelli-Steinberg, D.; Hunter, J. Metamerism, morphogenesis, and the expression of Carabelli and other dental traits in humans. *Am. J. Phys. Anthropol.* **2013**, *150*, 400–408. [CrossRef]

101. Atchley, W.R. Developmental quantitative genetics and the evolution of ontogenies. *Evolution* **1987**, *41*, 316–330. [CrossRef]

102. Bochdanovitz, Z.; de Jong, G. Antagonistic pleiotropy for life-history traits at the gene expression level. *Proc. R. Soc. Lond. B.* **2004**, *271*, S75–S78. [CrossRef]

103. Norry, F.M.; Vilardi, J.C.; Hasson, E. Negative genetic correlation between traits of the *Drosphila* head, and interspecific divergence in head shape. *Heredity* **2000**, *85*, 177–183. [CrossRef]

104. Riska, B. Some models for development, growth, and morphometric correlation. *Evolution* **1986**, *40*, 1301–1311. [CrossRef]

105. Jernvall, J. Mammalian molar cusp patterns: Developmental mechanisms of diversity. *Acta Zool. Fenn.* **1995**, *198*, 1–61.

106. Weiss, K.M. Duplication with variation: Metameric logic in evolution from genes to morphology. *Yearb. Phys. Anthropol.* **1990**, *33*, 1–23. [CrossRef]

107. Dahlberg, A.A. The evolutionary significance of the protostylid. *Am. J. Phys. Anthropol.* **1950**, *8*, 15–25. [CrossRef]

108. Bateson, W. *Materials for the Study of Variation: Treated with Special Regard to Discontinuity in the Origin of Species*; Macmillan and Company: London, UK, 1894. [CrossRef]

109. Butler, P.M. Comparison of the development of the second deciduous molar and first permanent molar in man. *Arch. Oral Biol.* **1967**, *12*, 1245–1260. [CrossRef]

110. Edgar, H.J.H.; Lease, L.R. Correlations between deciduous and permanent tooth morphology in a European American sample. *Am. J. Phys. Anthropol.* **2007**, *133*, 726–734. [CrossRef]

111. Farmer, V.; Townsend, G. Crown size variability in the deciduous dentition of South Australian children. *Am. J. Hum. Biol* **1993**, *5*, 681–690. [CrossRef]

112. Liversidge, H.M.; Molleson, T.I. Deciduous tooth size and morphogenetic field in the children from Christ Church, Spitalfields. *Arch. Oral Biol.* **1999**, *44*, 7–13. [CrossRef]

113. Bockmann, M.R.; Hughes, T.E.; Townsend, G.C. Genetic modeling of primary tooth emergence: A study of Australian twins. *Twin Res. Hum. Genet.* **2010**, *13*, 573–581. [CrossRef]

114. Edgar, H.J.H.; Ousley, S.D. Dominance in dental morphological traits: Implications for biological distance studies. In *Biological Distance Analysis*; Pilloud, M.A., Hefner, J.T., Eds.; Academic Press: London, UK, 2016; pp. 317–332. [CrossRef]